366.4-Gbit/s PCS-64QAM THz Transmission Enhanced by Likelihood-Aware Vector-Quantized Variational Autoencoders

Xiang Liu[(1,2)], Jiao Zhang[(1,2)*], Min Zhu[(1,2)*], Junhao Zhang[(1)] , Weidong Tong[(1,2)] , Yunwu Wang[(1,2)] , Zhigang Xin[(1,2)] , Bingchang Hua[(2)] , Mingzheng Lei[(2)] , Yuancheng Cai[(1,2)] , Jianjun Yu[(2,3)]

[(1)] National Mobile Communications Research Laboratory, Southeast University, Nanjing 210096, China
jiaozhang@seu.edu.cn; minzhu@seu.edu.cn
[(2)] Purple Mountain Laboratories, Nanjing, 211111, China
[(3)] Fudan University, Shanghai, 200433, China

Abstract *We present a novel likelihood-aware vector-quantized variational autoencoder for high-order PCS-QAM equalization and successfully demonstrate a dual-polarized 2 × 2 MIMO fiber-THz wireless system with a net rate of 366.4 Gbit/s using 40 Gbaud PCS-64QAM over a 20 km SSMF and 6.5 m wireless link.*

Introduction

Terahertz (THz, 300 GHz~10 THz) has emerged as a promising candidate for achieving ultra-high data rates in future 6G extreme connectivity [1]. Recently, several record-breaking transmission rates have been demonstrated in the THz-wave wireless system by employing photonics-assisted technologies [2]. The fiber-THz system enables seamless integration with high-speed optical fiber network, offering substantial application potential in the realm of 6G. Furthermore, advancement in the generation, modulation, and detection of THz signals has facilitated the seamless integration of THz wireless and optical networks [3-5].

Probabilistic constellation shaping (PCS) is a well-established technique that utilizes Maxwell-Boltzmann (M-B) distributions to generate signals with enhanced nonlinear resistance capacity [6]. However, conventional digital signal processing (DSP), such as the constant modulus algorithm (CMA) and radius-directed equalizer (RDE), are sub-optimal for the high-order PCS-QAM signals, which do not consider the likelihood of signals amplitude when updating the filter taps [7]. As an alternative to the CMA-based blind equalizer, the variational autoencoder (VAE) equalizers based on variational inference have been proposed [8-10]. While the VAE equalizer was generalized to cope with the high-order PCS-QAM signals and shown to be more performance than the CMA-based equalizers over the dual-polarized optical fiber channels, the approach is only available for channels that can be described in a simple form. However, many practical channels, including the non-ideal components, cannot be accurately well modelled. Consequently, the applicability of VAE-based equalizer is limited for the high-order PCS-QAM in the dual-polarized fiber-THz system.

In this work, we propose a novel likelihood-aware equalizer based on the vector quantized VAE (VQ-VAE) for high-order PCS-QAM signals, and successfully demonstrate a dual-polarized 2 × 2 MIMO THz wireless transmission system with a line rate of 462.4 Gbit/s and a net rate of 366.4 Gbit/s using 40 Gbaud PCS-64QAM modulation over 20 km SSMF and 6.5 m wireless link without the THz power amplifier.

Principle and experimental setup

Figure 1 shows the principle of VQ-VAE equalizer with a complex-valued 2 × 2 MIMO model. Fig. 2 depicts the experimental setup of our fiber-THz seamless integrated system with a dual-polarized 2 × 2 MIMO THz wireless link. The components are described as follows:

VQ-VAE equalization: Figure 1 visualizes the proposed probability-aware VQ-VAE equalization. In the fiber-THz system, the transmission channel $p_\theta(y|x)$ forms the VAE encoder, while the decoder $Q_\Phi(x|y)$ can infer x from y. The goal of variational inference is to learn the set of parameters Φ such that variational approximation $Q_\Phi(x|y)$ is closest to the true posterior $p(x|y)$. Therefore, finding the optimum variational approximation corresponds to finding the optimized equalizer for a fiber-THz transmission system. We implement our VQ-VAE using a pair of NNs, which have the ability to learn the nonlinear and complex relationships in data. In this work, we have a complex-valued 2 × 2 MIMO framework, which is suitable for the dual-polarization transmissions, as depicted in Fig. 3. The NNs equalizer takes the channel observation

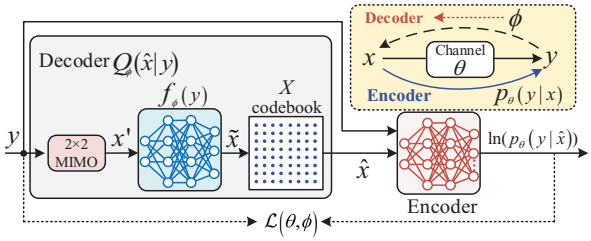

Fig. 1: Blind channel equalization and estimation using VQ-VAE with a complex-valued 2×2 MIMO model.

https://doi.org/10.1049/icp.2023.2474

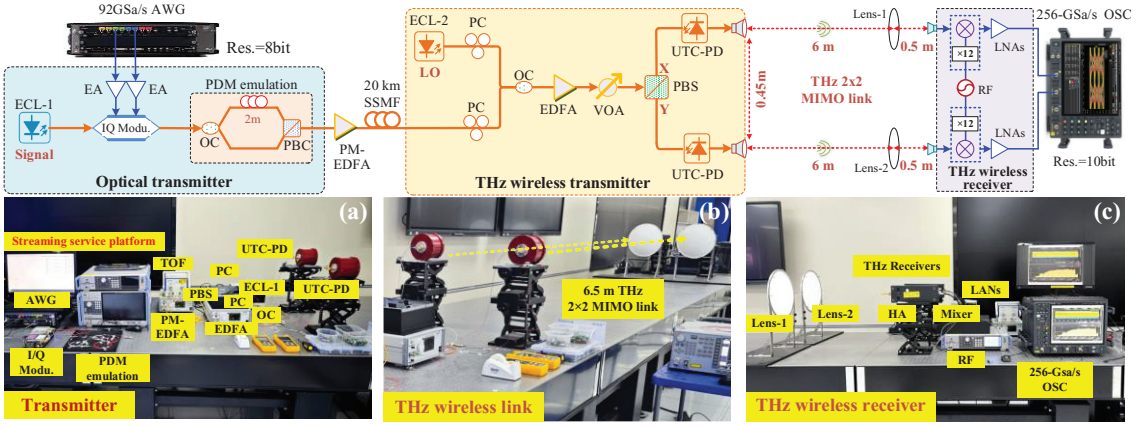

Fig. 2: The experimental setup of the fiber-THz seamless integrated system with a dual-polarized 2 × 2 MIMO wireless link, including the photos of (a) transmitter; (b) THz wireless link; (c) THz wireless receiver.

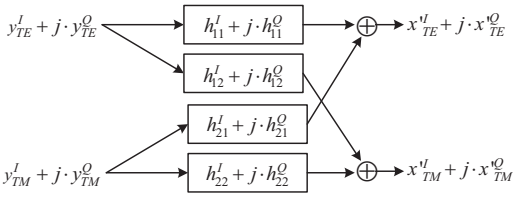

Fig. 3: A complex-valued 2×2 MIMO model in the VQ-VAE decoder $Q_\Phi(\hat{x}|y)$.

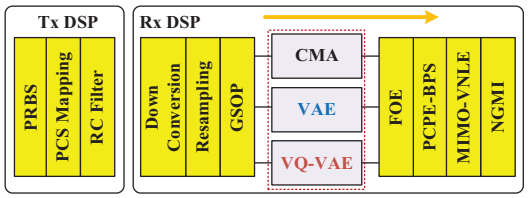

Fig. 4: Block diagram of Tx-side and Rx-side offline DSP.

x' as input and outputs a vector of equalized symbols $\tilde{x} = f_\Phi(y)$. It should be highlighted that in contrast to the conventional VAE-based method, the VQ-VAE decoder uses a codebook, which is identical to the constellation set X (M-QAM). The decoded symbol is obtained as $\hat{x} = \text{argmin}\|\tilde{x} - x\|$, $x \in X$. $Q_\Phi(\hat{x}|y)$ of the nonlinear equalizer and the demapper can be expressed as $Q_\Phi(\hat{x}|y) = 1$, $\hat{x} = \text{argmin}\|\tilde{x} - x\|$, which can be seen as a *one-hot* categorical distribution. VQ-VAE encoder can be interpreted as the channel estimator. During the VQ-VAE training, the expectation of likelihood-aware $E_{Q(x|y)}\{\ln(p_\theta(y|x))\}$ is evaluated. To train the VQ-VAE equalizer and estimator, we use the loss function $\mathcal{L}(\Phi, \theta) = -Eq_\Phi(x|y)\{\ln(p_\theta(y|x))\} + \rho\|\tilde{x} - \hat{x}\| = -\ln(p_\theta(y|\hat{x})) + \rho\|\tilde{x} - \hat{x}\|$. ρ is a hyperparameter that can be optimized to improve the convergence of the training model. The VQ-VAE jointly optimizes the parameters of the VAE encoder and decoder by minimizing $\mathcal{L}(\Phi, \theta)$. Upon convergence, the VQ-VAE decoder $Q_\Phi(\hat{x}|y)$ can be viewed as an optimized equalizer in the fiber-THz system.

Experimental setup: In the transmitter offline DSP, a single carrier signal X is modulated by a 92-Gsa/s arbitrary waveform generator (AWG) and amplified by the 40-GHz electrical amplifiers (EAs) before driving a 35-GHz I/Q modulator. Polarization-division multiplexing uses a fiber delay emulator with a 2 m decorrelation delay. The baseband optical signal is amplified by a polarization-maintaining erbium doped fiber amplifier (EDFA). Over a 20 km SSMF with an average loss of 0.2 dB/km, the optical signal and ECL-1 as local oscillator (LO) are coupled by an optical coupler (OC) and amplified by an EDFA. A polarization beam splitter (PBS) is employed to split combined lightwaves into two polarizations, which are then up-converted to the THz signal by UTC-PD. Polarization controllers (PCs) maximize optical power into polarization-sensitive UTC-PD. Two parallel THz signals from the UTC-PDs are delivered over a 6.5 m 2 × 2 MIMO wireless link. Two lenses are deployed to maximize received signal power. THz-wave signal is received with two parallel horn antennas (HAs) with WR-2.2 waveguide interfaces. THz receiver is driven by electronic LO source to implement analog down conversion, and each has a mixer and a × 12 frequency multiplier. At the receiver, IF signal is boosted by a pair of low-noise amplifiers (LNAs) and captured by the 256-Gsa/s digital storage oscilloscope (OSC) with a 59-GHz bandwidth. In receiver offline DSP, the captured signals are down-converted and resampled to two samples per symbol, squaring time recovery. In this work, we implement the polarization demultiplexing and equalization of dual-polarized signals with three different methods, as shown in Fig. 4. The step of frequency offset estimation (FOE) removes the residual frequency offset of the received signal. We employ a principal component-based phase estimation (PCPE) stage and blind phase search (BPS) stage [11] for the phase noise estimation. A second-order Volterra nonlinear equalizer with MIMO (MIMO-VNLE) is used to compensate for I/Q imbalance and nonlinear impairment in the fiber-THz wireless transmission system. Finally, the NGMI value can be calculated.

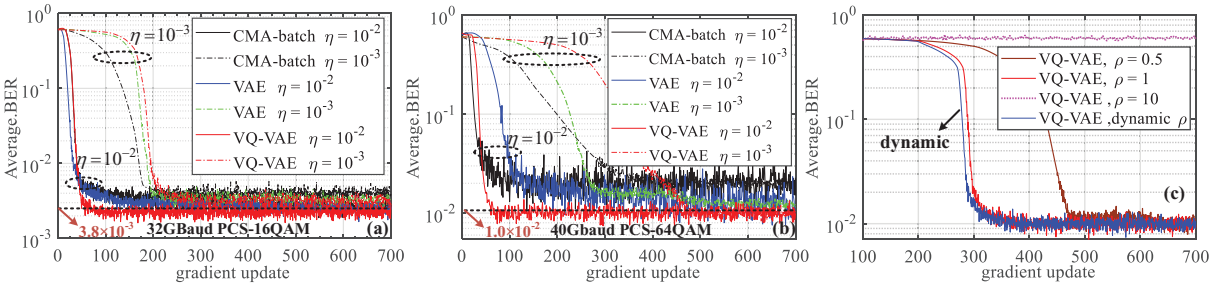

Fig. 5: Convergence behavior of three channel equalizers with different learning rates at 12 dBm input power. (a) for 32Gbaud PCS-16QAM; (b) for 40Gbaud PCS-64QAM; (c) the optimized hyperparameter ρ.

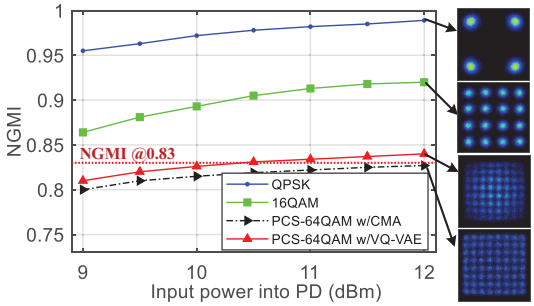

Fig. 6: NGMI of received 40 Gbaud QPSK, 16QAM, 64QAM and PCS-64QAM signals as well as recovered constellation.

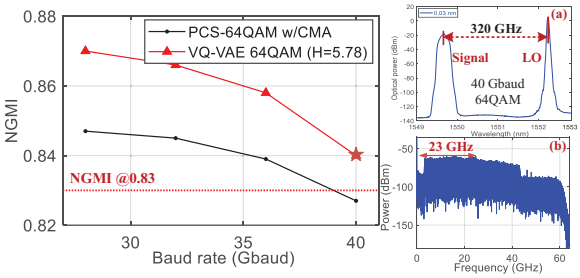

Fig. 7: NGMI versus baud rate for uniform and VQ-VAE PCS-64QAM after a 20 km SSMF and 6.5 m wireless link.

Results and Discussion

We examine the effectiveness of the VQ-VAE by considering different equalizers, as shown in Fig. 5. The number of transmitted symbols is 262144, the training dataset contains 32768 symbols, and the learning rate is η = 0.01, 0.001.

Figure 5 shows the average BER curves of three training equalizers, including CMA-batch, VAE, and VQ-VAE, for PCS-16, 64QAM signals, respectively. For considered configurations, we observe that: (i) The VQ-VAE-based approaches proposed in this work is more robust to variations in modulation orders and learning rates. (ii) For high-order signals, a large learning rate generally leads to a faster convergence for all considered equalizers, except for the CMA-based schemes, which suffers from training instability. (iii) There is an optimal value that can balances performance against convergence speeds and computational complexity. The VQ-VAE approach requires the fewest gradient updates to converge to optimal performances. The impact of the hyperparameter ρ on the VQ-VAE training is also analysed, as shown in Fig. 5(c). It is shown that for ρ = 1, more gradient updates are required to convergence compared to ρ = 0.5. However, for ρ = 10, the VQ-VAE equalizer fails to converge. We can find the optimal ρ, as depicted in Fig. 5(c).

Figure 6 shows the measured NGMI of the received 40Gbaud QPSK, 16QAM, 64QAM and PCS-64QAM signals after 20 km SSMF and 6.5 m wireless delivery versus input power into a PD. At 0.83 NGMI threshold, the required input power into the PD for VQ-VAE PCS-64QAM signals is 10.4 dBm, while for the CMA-based PCS-64QAM signal transmission cannot reach 0.83 threshold. It also shows the constellation diagrams of QPSK, 16QAM, 64QAM, and PCS-64QAM symbols after recovery at the optimal input power.

Figure 7 depicts the highest rate for the PCS-64QAM signal transmission that can be achieved is 40 Gbaud at the 0.83 NGMI threshold. Fig. 7(a) shows the optical spectrum of 40Gbaud 64QAM optical signal and optical LO with a 320 GHz frequency space. Fig. 7(b) gives the electrical spectrum of 40 Gbaud PCS-64QAM IF signal. By employing a dual-polarized VQ-VAE-based PCS-64QAM signal transmission, a line rate of 462.4 Gbit/s (5.78 × 40 × 2 = 462.4 Gbit/s) can be achieved at 0.83 NGMI threshold. With SD-FEC with 25% overhead, the net rate is 366.4 Gbit/s ([5.78 – 6 × (1 – 0.8)] × 40 × 2 = 366.4 Gbit/s).

Conclusions

We propose a novel likelihood-aware VQ-VAE equalizer for PCS-QAM signals transmission and successfully demonstrate a dual-polarized fiber-THz 2 × 2 MIMO transmission system with a line rate of 462.4 Gbit/s using 40 Gbaud PCS-64QAM modulation over 20 km SSMF and 6.5 m wireless delivery, without THz power amplifier. Advanced nonlinear algorithm for the PCS signal can break through the SNR limitation, facilitating ultra-high rate transmission, which is suitable for evaluating the complex channel and designing constellation shaping for emerging services.

Acknowledgements: This research was supported in part by the National Natural Science Foundation of China (62101121, 62101126, 62201397, 62201393, 62271135), the project funded by China Postdoctoral Science Foundation (2021M702501, 2022T150486).

References

[1] M. Zhu, J. Zhang, B. Hua, et al., “Ultra-wideband fiber-THz-fiber seamless integration communication system toward 6G: architecture, key techniques, and testbed implementation,” *Science China Information Sciences*, vol. 66, no. 1, pp. 113301, 2023, DOI: 10.1007/s11432-022-3565-3.

[2] S. Jia, M.C. Lo, L. Zhang, et al, “Integrated dual-laser photonic chip for high-purity carrier generation enabling ultrafast terahertz wireless communications,” *Nature communications*, vol. 13, no. 1, pp. 1388, 2022, DOI: 10.1038/s41467-022-29049-2.

[3] J. Zhang, M. Zhu, M. Lei, et al, “Real-time demonstration of 103.125-Gbps fiber–THz–fiber 2× 2 MIMO transparent transmission at 360–430 GHz based on photonics,” *Optics letters*, vol. 47, no. 5, pp. 1214-1217, 2022, DOI: 10.1364/OL.448064.

[4] J. Zhang, M. Zhu, B. Hua, et al, “Real-time Demonstration of 100 GbE THz-wireless and Fiber Seamless Integration Networks,” *Journal of Lightwave Technology*, vol. 41, no. 4, pp. 2022, DOI: 10.1109/JLT.2022.3204268.

[5] S. Jia, L. Zhang, S. Wang, et al., “2× 300 Gbit/s line rate PS-64QAM-OFDM THz photonic-wireless ransmission,” *Journal of Lightwave Technology*, vol. 38, no. 17, pp. 4715-4721, 2020, DOI: 10.1109/JLT.2020.2995702.

[6] F. R. Kschischang, S. Pasupathy, “Optimal nonuniform signaling for Gaussian channels,” *IEEE Transactions on Information Theory*, vol. 39, no. 3, pp. 913-929, 1993, DOI: 10.1109/18.256499.

[7] J. Ding, M. Wang, W. Li, et al, “Wireless transmission of a 200-m PS-64QAM THz-wave signal using a likelihood-based selection radius-directed equalizer,”. *Optics Letters*, vol. 47, no. 15, pp. 3904-3907, 2022, DOI: 10.1109/18.256499.

[8] V. Lauinger, F. Buchali, L. Schmalen, “Blind equalization and channel estimation in coherent optical communications using variational autoencoders,” *IEEE Journal on Selected Areas in Communications*, vol. 40, no. 9, pp. 2529-2539, 2022, DOI: 10.1109/JSAC.2022.3191346.

[9] A. Caciularu, D. Burshtein, “Blind channel equalization using variational autoencoders,” in *IEEE International Conference on Communications Workshops (ICC Workshops)*, pp. 1-6, 2018, DOI: 10.1109/ICCW.2018.8403666.

[10] M. A. Alawad, M. Q. Hamdan, K. A. Hamdi, et al, “A New Approach for an End-to-end Communication System Using Variational Auto-encoder (VAE),” in *IEEE Global Communications Conference*, pp. 5159-5164, 2022, DOI: 10.1109/ICCW.2018.8403666.

[11] J. Ding, W. Li, Y. Wang, et al., “124.8-Gbit/s PS-256QAM Signal Wireless Delivery over 104 m in a Photonics-aided Terahertz-Wave System,” *IEEE Transactions on Terahertz Science and Technology*, vol. 12, no. 4, pp. 409-414, 2022, DOI: 10.1109/TTHZ.2022.3164356.